arXiv:physics/0503092v1 [physics.atm-clus] 11 Mar 2005

Electronic structure of clusters $(\mathrm{LiBC})_n$: $n = 1$, 2 and 4

G. M. Lombardo, [a] A. Grassi, [a] G. Forte, [a] G. G. N. Angilella, [b]
R. Pucci, [b] and N. H. March [c,d]

[a] *Dipartimento di Scienze Chimiche, Facoltà di Farmacia, Università di Catania,*
Viale A. Doria, 6, I-95126 Catania, Italy

[b] *Dipartimento di Fisica e Astronomia, Università di Catania, and*
Istituto Nazionale per la Fisica della Materia, UdR Catania,
Via S. Sofia, 64, I-95123 Catania, Italy

[c] *Department of Physics, University of Antwerp,*
Groenenborgerlaan 171, B-2020 Antwerp, Belgium

[d] *Oxford University, Oxford, UK*

Received 2 February 2008

Abstract

A crystalline form of LiBC is known which has been predicted to be superconducting, with a T_c comparable to that of MgB_2. In both compounds, superconductivity is enhanced by the presence of two electronic bands, one of which is close to a dimensional crossover. Here, we take a quantum chemical approach, and investigate the structural and electronic properties of small clusters $(\mathrm{LiBC})_n$ ($n = 1-4$). With increasing cluster size, we find that several properties of crystalline LiBC evolve naturally from the corresponding properties of the clusters. In particular, one may recognize the origin of the solid bilayered structure, typical of magnesium diboride, and the character of the electronic σ-band, arising from the overlap of the atomic orbitals in the in-plane BC rings. Two aspects especially emphasized are *(a)* the HOMO-LUMO gap as function of n and *(b)* the role of different spin multiplicity.

PACS: 36.40.Mr, 36.40.Cg, 74.70.Ad

A crystalline form of hole-doped LiBC has been studied, which has been predicted to be superconducting with a transition temperature T_c comparable to that of the isoelectronic compound MgB_2 [1,2]. The structure of LiBC is closely related to the bilayered structure of MgB_2, with Li replacing Mg, and B_2 being replaced by BC, but with hexagonal BC layers alternating so that B is nearest neighbour to C both within the in-plane rings, and along the c axis. Although the number of valence electrons decreases by one in replacing Mg with Li, this is compensated by the substitution of B_2 by BC. At variance with its similarities with MgB_2, a distinctive feature of LiBC is that the Li content in Li_xBC can be varied with respect to its stoichiometric value $x = 1$, without any appreciable change of crystalline structure for a quite wide range in $x = 0.24 - 1$ [1], thus allowing to study the superconducting properties of this material upon self-hole-doping.

Both MgB_2 and LiBC are characterized by a similar electronic structure, with a three-dimensional (3D) σ subband, mainly arising from the B_2 (respectively, BC) layers, and a quasi-bi-dimensional (quasi-2D) π subband, mainly arising from the electrons delocalization across the layers. The relevance of the proximity of the π subband to a 3D–2D crossover, *i.e.* an electronic topological transition, for the dependence of T_c and of the isotope exponent on doping has been emphasized elsewhere within the two-band model of superconductivity [3].

Thus, it would be natural to think of both structural and electronic properties of crystalline LiBC as arising from the underlying structural and electronic properties of the individual LiBC units. This has motivated the present study of the electronic structure of the small clusters $(\mathrm{LiBC})_n$, with n going from 1 to 4. With increasing cluster size n, the solid crystalline and electronic structure of LiBC can be approached, thus allowing one to recognize the origin of the peculiar bilayered structure of the diborides, and the nature of their two coupled electronic bands. The present study shows that such features are already present in clusters $(\mathrm{LiBC})_n$, with n as small as 4.

For these clusters the electronic stuctures, optimized geometries, and the vibrational analysis were obtained using the GAUSSIAN 03 package [4], with *ab initio* self-consistent field Hartree-Fock wavefunctions at the 6-311+G(d) level of the theory (including polarization and diffuse functions). Each cluster was studied with various spin multiplicities depending on the number of possible uncoupled valence electrons. Here, we report only those which attained a true minimum.

At this level of accuracy of the electronic structure studies, we show in Fig. 1 the fully optimized geometrical configuration of LiBC for different spin multiplicities. Table 1 records the equilibrium bond lengths for Li–Li, Li–C, Li–B, and B–C, for some of the clusters considered in this study.

One of the focal points of the present letter is the HOMO-LUMO energy gap ϵ_{HL} of the various clusters considered. Therefore in Fig. 2 for $n = 1$ this gap is recorded for the three spin multiplicities studied. There is not a huge spread of ϵ_{HL} for $n = 1$ with spin multiplicity, but the smallest gap is when this quantity is ~ 5. The corresponding total Hartree-Fock energies are given in Tab. 2 for the three different spin multiplicities.

Turning to the case $n = 2$, two geometries are shown in Figs. 3a and 3b, with the relevant equilibrium bond lengths recorded in Tab. 1. The 'trans' configuration of Fig. 3, with multiplicity 3, has the lowest energy at the present level of approximation. The corresponding energy gaps for the two configurations are seen not to be very different, with also a relatively weak dependence on spin multiplicity.

The largest cluster studied here corresponds to $n = 4$. Fig. 4 shows the fully optimized configurations of the four isomer quadruplet $(\mathrm{LiBC})_4$ clusters. The top row of this Figure has C_{2v} symmetry, whereas the lower Figure symmetry is C_1. Studying stability via the normal mode vibrational frequencies, we find that some frequencies of the extreme right symmetry cluster in the top row of Fig. 4 are imaginary, all the other isomers presented here being stable in this context.

It is appropriate at this point to briefly discuss the geometry of the $(\mathrm{LiBC})_4$ clusters in relation to the crystalline solid form. The main point to emphasize is that in Fig. 4 the three configurations for which the vibrational frequencies are all real each contain a six-membered ring, consisting of alternating boron and carbon atoms. However, orthogonal to the ring, each configuration has a Li dimer passing through the centre of the ring. Turning to the solid-state structure, Fig. 1 of Ref. [1] contains two such BC hexagons again, which are intercalated by Li layers. It should be stressed that adjacent hexagons in the solid have no direct B–B or C–C bonds. One discerns a Li–Li axis passing through the centre of the BC hexagons, establishing thereby close contact with the cluster structures already discussed. From Table 1, one indeed finds that the Li–Li distances range between 3.30 and 3.60 Å, to be compared and contrasted with the interlayer Li–Li distance in solid LiBC, which is of 3.529 Å [1].

Another analogy with the solid phase is provided by the electronic charge distribution in the largest clusters examined in this study. Fig. 5 therefore shows the Mulliken density charge isosurfaces of the valence electrons, for the $(\mathrm{LiBC})_4$ cluster with C_1 symmetry (Fig. 4). One may detect the formation of a ring of electronic charge piling between the C and B atoms, which preludes to the σ band in solid LiBC [1].

Fig. 2 shows both a substantial lowering of the energy gap ϵ_{HL} with increase in cluster size as well as a substantial spread in the values obtained for spin multiplicity 9 for the four geometries depicted in Fig. 4. It is also of interest to note that the dimer $(\mathrm{LiBC})_2$ binding energy measured relative to the energy of the two separated LiBC units is found from Table 2 to be ~ 4 eV.

In conclusion, by using quantum chemical techniques, we have studied the *Aufbau* of crystalline LiBC by gathering individual LiBC units into small

$(LiBC)_n$ clusters. In particular, we focussed on the structure optimization and the computation of selected electronic properties, such the HOMO-LUMO gap as a function of n and the Mulliken charge density distribution of the largest cluster considered here ($n = 4$), which may provide insight into the salient properties of crystalline LiBC. Already for $n = 4$ we can recognize the formation of alternating BC rings, with significant overlap of the valence electrons along the ring, and comparably less electron delocalization in the direction perpendicular to the ring, along which a Li–Li dimer is favoured to align. This is reminiscent of the bilayered structure of crystalline LiBC, and of its two-band electronic character, whose relevance for superconductivity is well-known.

References

[1] H. Rosner, A. Kitaigorodsky, W. E. Pickett, Prediction of high T_c superconductivity in hole-doped LiBC, Phys. Rev. Lett. 88 (2002) 127001.

[2] J. K. Dewhurst, S. Sharma, C. Ambrosch-Draxl, B. Johansson, First-principles calculation of superconductivity in hole-doped LiBC: $T_c = 65$ K, Phys. Rev. B 68 (2003) 020504(R).

[3] G. G. N. Angilella, A. Bianconi, R. Pucci, Multiband superconductors close to a 2D–3D electronic topological transition, J. Supercond., accepted for publication ... (2005) ...

[4] M. J. Frisch, G. W. Trucks, H. B. Schlegel, G. E. Scuseria, M. A. Robb, J. R. Cheeseman, V. G. Zakrzewski, J. A. Montgomery, Jr., R. E. Stratmann, J. C. Burant, S. Dapprich, J. M. Millam, A. D. Daniels, K. N. Kudin, M. C. Strain, O. Farkas, J. Tomasi, V. Barone, M. Cossi, R. Cammi, B. Mennucci, C. Pomelli, C. Adamo, S. Clifford, J. Ochterski, G. A. Petersson, P. Y. Ayala, Q. Cui, K. Morokuma, D. K. Malick, A. D. Rabuck, K. Raghavachari, J. B. Foresman, J. Cioslowski, J. V. Ortiz, A. G. Baboul, B. B. Stefanov, G. Liu, A. Liashenko, P. Piskorz, I. Komaromi, R. Gomperts, R. L. Martin, D. J. Fox, T. Keith, M. A. Al-Laham, C. Y. Peng, A. Nanayakkara, C. Gonzalez, M. Challacombe, P. M. W. Gill, B. Johnson, W. Chen, M. W. Wong, J. L. Andres, C. Gonzalez, M. Head-Gordon, E. S. Replogle, J. A. Pople, Gaussian 03, Revision B05 (2003-12-16), Gaussian, Inc., Pittsburgh PA (2003).

Acknowledgements

GGNA wishes to thank the Department of Physics, University of Antwerp, where this work was brought to completion, for warm hospitality and for the stimulating environment. NHM acknowledges that his contribution to this study was made during a visit to the University of Catania. He wishes to thank the Department of Physics and Astronomy for generous support.

Table 1
Various equilibrium bond lengths (in Å) for some of the clusters considered in this study.

	LiBC	LiBC	LiBC	(LiBC)$_2$	(LiBC)$_2$ trans	(LiBC)$_2$	(LiBC)$_2$ trans	(LiBC)$_4$ C$_{2v}$ (1)	(LiBC)$_4$ C$_{2v}$ (2)	(LiBC)$_4$ C$_1$
S	1	3	5	1	1	3	3	9	9	9
Li–Li				3.122282	4.245581	3.0483	4.253679	3.353511	3.559604	3.300477
Li–C	1.9624	1.9103	1.9078	2.26	2.1502	2.298	2.4106	2.343600	2.646053	2.297274
				2.2568	2.1433	2.2981	2.1345	2.215844	2.22583	2.266067
				2.4572	2.4293	2.6453	2.0751	2.215844	2.22583	2.218518
				2.1353	4.6509	2.1503	4.1552	2.3436	2.646053	2.292753
								2.215844	2.22583	2.265326
								2.215844	2.22583	2.223154
								2.522509	2.02507	2.316641
								2.522509	2.02507	1.940265
									2.476577	2.217949
									2.476577	
Li–B	1.9624	3.289	2.2398	2.4814	2.574	3.0006	3.3345	2.146662	2.261255	2.213358
				2.4838	2.1849	3.0007	2.1358	2.146662	2.29926	2.274297
				2.2551	2.1058	2.1078	2.1539	2.268792	2.261255	2.260106
				2.2543	3.2111	2.1078	2.8393	2.289784	2.261255	2.210945
								2.268792	2.29926	2.274707
								2.268792	2.261255	2.260612
								2.289784	2.45892	2.211303
								2.268792	2.45892	2.157141
								2.329519		2.331481
								2.329519		
B–C	1.3944	1.3787	1.6026	1.4185	1.4066	1.3508	1.4131	1.530041	1.489521	1.496576
				3.2822	4.0533	3.8477	4.1366	1.546234	1.485995	1.567349
				1.3999	1.4091	1.4583	1.3942	1.499536	1.473746	1.484584
				1.4186	1.4496	1.3868	1.4616	1.534722	1.515207	1.529249
								1.534722	1.515207	1.516692
								1.571215	1.63323	1.653384
								1.546234	1.485995	1.620702
								1.499536	1.473746	1.49723

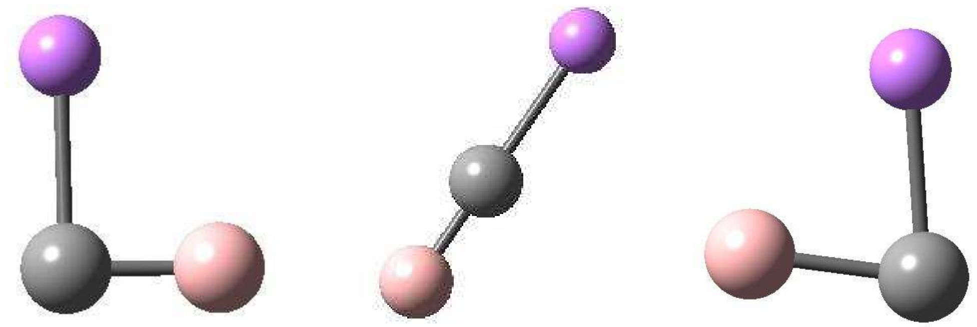

$S = 1$ $S = 3$ $S = 5$

Fig. 1. Fully optimized configuration of the LiBC singlet cluster for $S = 1$, 3, 5 (left to right; Li: purple; B: pink; C: grey).

Table 2
Calculated properties of $(\mathrm{LiBC})_n$ clusters. All energies are in hartrees.

n	S		E_{HF}	E_{HF}/n	α-HOMO	α-LUMO	β-HOMO	β-LUMO
1	1		−69.77	−69.77	−0.31	−0.01	−0.31	−0.01
1	3		−69.85	−69.85	−0.28	−0.01	−0.27	−0.01
1	5		−69.77	−69.77	−0.23	0.00	−0.34	−0.01
2	1		−139.81	−69.905	−0.29	0.00	−0.29	0.00
2	1	trans	−139.81	−69.91	−0.28	−0.01	−0.28	−0.01
2	3		−139.84	−69.92	−0.28	0.00	−0.27	0.00
2	3	trans	−139.85	−69.92	−0.30	0.00	−0.28	−0.01
4	9	C_{2v} (1)	−279.69	−69.92	−0.17	0.00	−0.26	0.00
4	9	C_{2v} (2)	−279.69	−69.92	−0.11	−0.02	−0.30	0.00
4	9	C_{2v} (3)	−279.73	−69.93	−0.22	0.00	−0.24	0.00
4	9	C_1	−279.73	−69.93	−0.19	0.00	−0.25	0.00

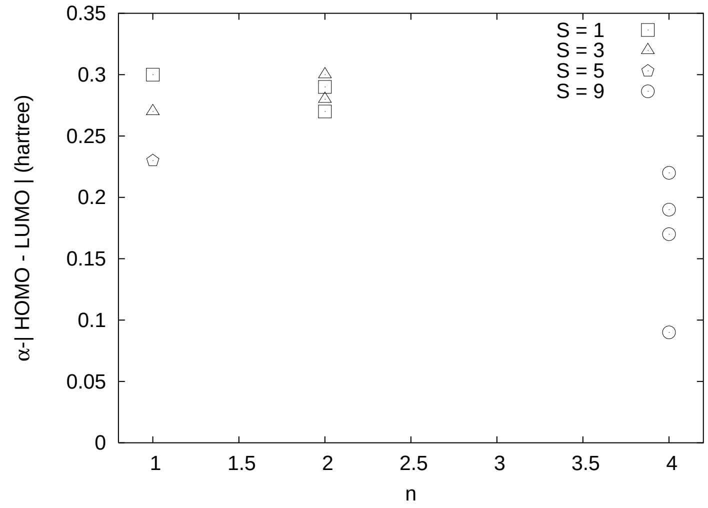

Fig. 2. HOMO-LUMO gap in the $(\mathrm{LiBC})_n$ clusters as a function of n. Different symbols refer to the different spin multiplicity.

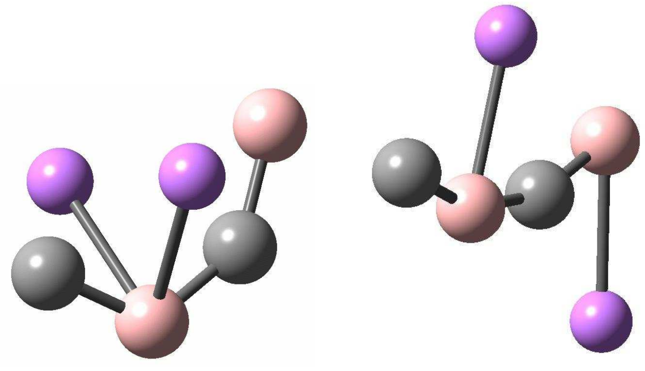

$S = 1$ $\quad$ $S = 1$ (trans)

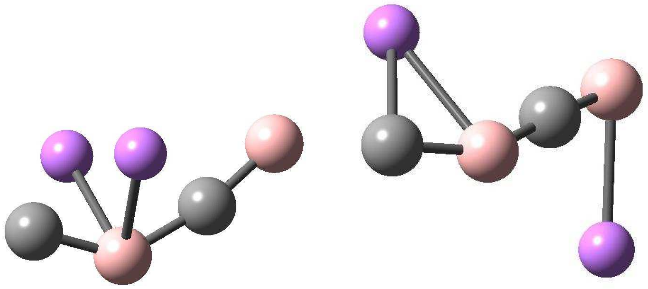

$S = 3$ $\quad$ $S = 3$ (trans)

Fig. 3. *(a), top row:* Fully optimized configurations of the two isomer singlet $(\mathrm{LiBC})_2$ clusters. *(b), bottom row:* Fully optimized configurations of the two isomer triplet $(\mathrm{LiBC})_2$ clusters.

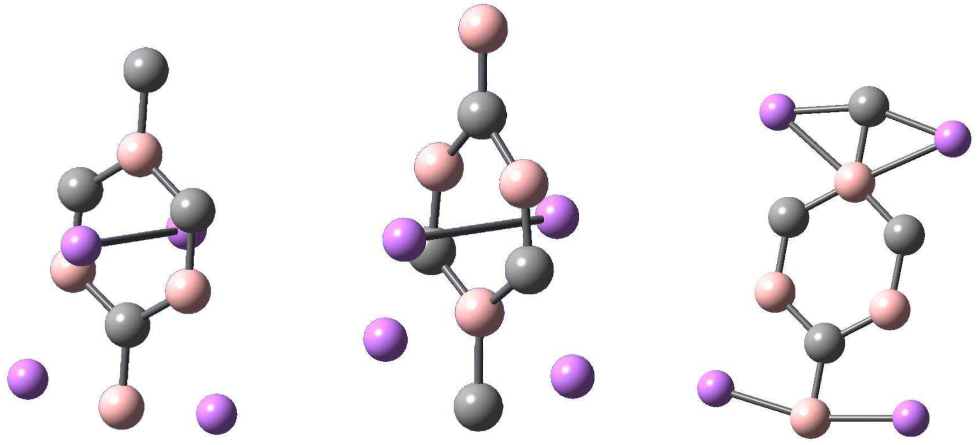

$S = 9$, C$_{2v}$ (1) $S = 9$, C$_{2v}$ (2) $S = 9$, C$_{2v}$ (3)

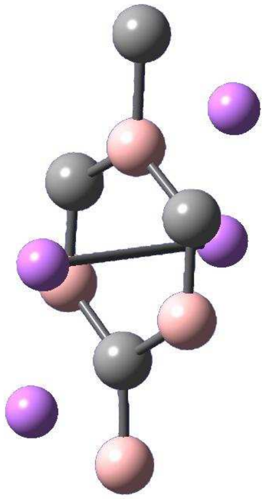

$S = 9$, C$_1$

Fig. 4. Fully optimized configurations of the four isomer quadruplet (LiBC)$_4$ clusters with C$_{2v}$ symmetry (top row) and C$_1$ symmetry (bottom). Some of the frequencies of the C$_{2v}$ (3) are imaginary, the other three isomers shown being stable.

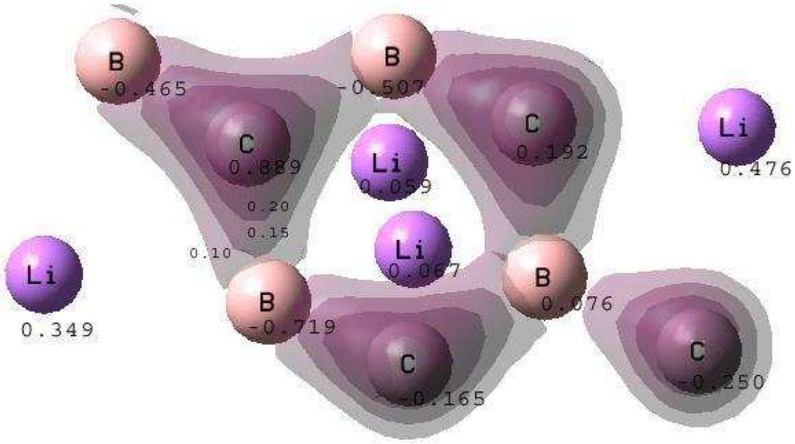

Fig. 5. Isosurfaces of the valence electron density for the $(LiBC)_4$ cluster with C_1 symmetry in Fig. 4. Each isosurface is labeled with the relative value of the electron density $(0.10 - 0.20)$, while each atom is labeled with its Mulliken atomic charge.